READ 2024
RESEARCH & EDUCATION IN AIRCRAFT DESIGN
WARSAW, POLAND | 6-8 NOVEMBER 2024

OPTIMAL CONTROL IN THE TRANSITION PHASE OF AN EVTOL UAV IN A HYBRID CONFIGURATION

Katarzyna Pobikrowska[1] & Tomasz Goetzendorf-Grabowski[1]

[1]Warsaw University of Technology (WUT), Institute of Aeronautics and Applied Mechanics, Nowowiejska 24, 00-665 Warsaw, Poland

Abstract

Recent years have seen a notable increase in the popularity of contemporary eVTOL aircraft, both in academic and commercial contexts. However, the high energy consumption of vertical propulsion systems represents a significant challenge. Insufficient energy density of batteries on the market hinders the endurance of vertical flying aircraft, therefore a need for energy-optimal solutions arises. It is postulated that optimizing the trajectory of the transition phase is a viable option in mitigating the above shortcomings. The transition of a VTOL aircraft consist of accelerating from hovering to forward flight, at which point the full lift force is provided by the wings, instead of the vertical propulsion. The following paper presents the results of a study in which the trajectory of an electric VTOL UAV has been optimized using methods of direct numerical optimal control. As a test case, a quad-plane VTOL aircraft was selected as being one of the most popular configurations on the market. One of the most pronounced benefits of the configuration is that it is easy to retrofit a fixed-wing aircraft by enhancing it with vertical flight propulsion system to maintain the high endurance in forward flight. The Optimal Control Problem (OCP) has been posed on the basis of a numerical model of the quad-plane VTOL UAV motion, as well as a set of constraints on the state and control variables. The mentioned model includes the aerodynamic models of aircraft body, and the propulsion system. The OCP has been solved with a nonlinear programming solver IPOPT to yield a feasible, energy-optimal trajectory during which the aircraft performs a fast and aggressive pitch down maneuver to complete the transition phase. The resulting trajectory profile shows a reduction in energy consumption of up to 70% in comparison to a zero pitch reference case. Findings show that the best results are achieved not only in a proper propulsion control but also in reducing the time spent in the high power, transition regime. The saved energy can lead to higher endurance of the drone, a smaller battery and a more efficient usage of onboard resources, which is an important consideration for the feasibility and usability of eVTOL drones in today's world and in the future.

Keywords: optimal control, trajectory optimization, LQR, VTOL, UAV

1. Introduction

In recent years, there has been a notable increase in the popularity of unmanned aerial vehicles (UAVs) within the field of aviation. This interest is shared by professionals, academics as well as those engaged in recreational activities. The unmanned drone, in its various shapes and forms, serves to replace dangerous, repetitive and boring operations [1] in a shorter time and at a lower cost than manned aircraft [2]. Additionally, there has been a notable rise in the number of new companies and investments in the private and public sectors, as evidenced by the findings of NexUAV [3]. Furthermore, the advent of the new UAV market is stimulating innovation, introducing novel concepts and fostering growth in academia. New applications for all types of unmanned aircraft are being developed on a continuous basis, including surveillance, military, medical, agricultural, scientific research and exploration, disaster relief, wildlife, fire and international border monitoring, among others [4, 5]. In many of these areas, it is beneficial for the vehicle to have vertical lift capabilities, which render it

useful in smaller and more confined spaces without a runway [6]. Moreover, a considerable number of applications necessitate the aircraft's capacity to hover. It can be reasonably concluded that a significant proportion of the UAV market will be accounted for by vertical take-off and landing (VTOL) and hybrid vehicles. A hybrid vehicle is a combination of fixed-wing and rotary-wing systems, which can potentially fulfil a wider range of applications. However, the benefits are offset by the high energy consumption during the vertical phases of flight. The energy requirements of VTOL aircraft have provided motivation to search for energy-saving solutions, whether in the design of drones [6–8], or mission planning [9]. Similarly, hybrid aircraft, which are derived from rotorcraft, are confronted with comparable challenges in this regard. Such aircraft, which are typically equipped with distributed propulsion systems, stand to gain considerably from the deployment of electric motors for thrust generation. Electric propulsion, excluding the energy storage system, is an efficient, lightweight, robust, fast and easy-to-use technology. The principal challenge is the lack of adequate electrical power on board. There are numerous potential solutions to this problem, including the use of fuel cells or the integration of an internal combustion engine alongside vertical electric propulsion. These approaches have demonstrated considerable promise and have been successfully employed in practice. However, the research presented in this paper adopts a distinct strategy, focusing on the reduction of energy consumption through the meticulous planning of the vehicle's motion and control.
Having the mentioned arguments in mind, this paper proposes a way to increase the vehicle endurance without the need to redesign the aircraft or changes in payload mass by reducing the energy consumption. The approach is based solely on shaping the flight trajectory of the vehicle in an energy-optimal manner. In order to achieve this objective, optimal control theory has been selected, as the trajectory that results from solving an optimal control problem (OCP) is guaranteed to be feasible based on the mathematical model of the vehicle motion, as well as any requirements and constraints on the trajectory profile. A similar approach, with the difference of using a single polynomial to describe and optimize one state variable - the pitch angle was studied in [10]. The paper showed quite significant benefits in reducing the energy consumption through optimization of the transition phase, even under more restricting assumptions on the shape of the trajectory.

2. Optimal transition scenario

The VTOL type that was subjected to analysis in this study is the quad-plane, which incorporates a quad-copter with a fixed-wing aeroplane. This hybrid VTOL approach enables the achievement of longer flight times in comparison to the quad-copter, while still allowing vertical flight. Furthermore, the distinct vertical and horizontal propulsion systems result in a greater number of motors and propellers compared to alternative configurations. This fact results in added redundancy and increased safety of the vehicle [11]. In addition to enhancing safety, the quad-plane allows for return and landing even in situations where the vertical propulsion is lost or the battery capacity is low. The aircraft's geometry can be optimised exclusively for forward flight (e.g. increasing stability, endurance, and decreasing drag) due to the relatively small influence of the vertical propulsion on forward flight aerodynamics when compared with other hybrid VTOL aircraft types [12].
A quad-plane, like every other hybrid VTOL vehicle, has distinct flight phases. Its flight profile usually can be described as follows. After take-off, the aircraft must gain altitude to a safe height to enable the execution of further manoeuvres. Subsequently, during the transition phase, the aircraft is required to accelerate to a minimum of stall speed. This is accompanied by a gradual replacement of the thrust provided by the propellers with lift generated by the wings. Subsequently, the aircraft accelerates further in forward flight until it reaches the designated cruise speed. A comparable procedure is repeated in instances where the aircraft is anticipated to decelerate to a hover or to land. The trajectory in transition is dependent on pilot pitch and roll inputs and automated to achieve the desired values [13]. An obvious, simple scenario for transition is the zero-pitch transition, in which the forward acceleration is provided solely by the pusher propeller, while the vertical propulsion maintains altitude.
As might be expected, the potential for energy savings in hover or forward flight is limited for a vehicle that has already been designed. In hover, the energy consumed is dependent on the weight of the vehicle, the efficiencies of the system, and any disturbances, for example due to weather. In forward flight, the aircraft geometry has already been optimised for cruise conditions. Moreover, the energy

requirements for horizontal flight propulsion are low. Therefore, it is postulated, that the greatest savings can be achieved by carefully designing the course of the transition phase by modifying the reference trajectory.

2.1 Mathematical Model

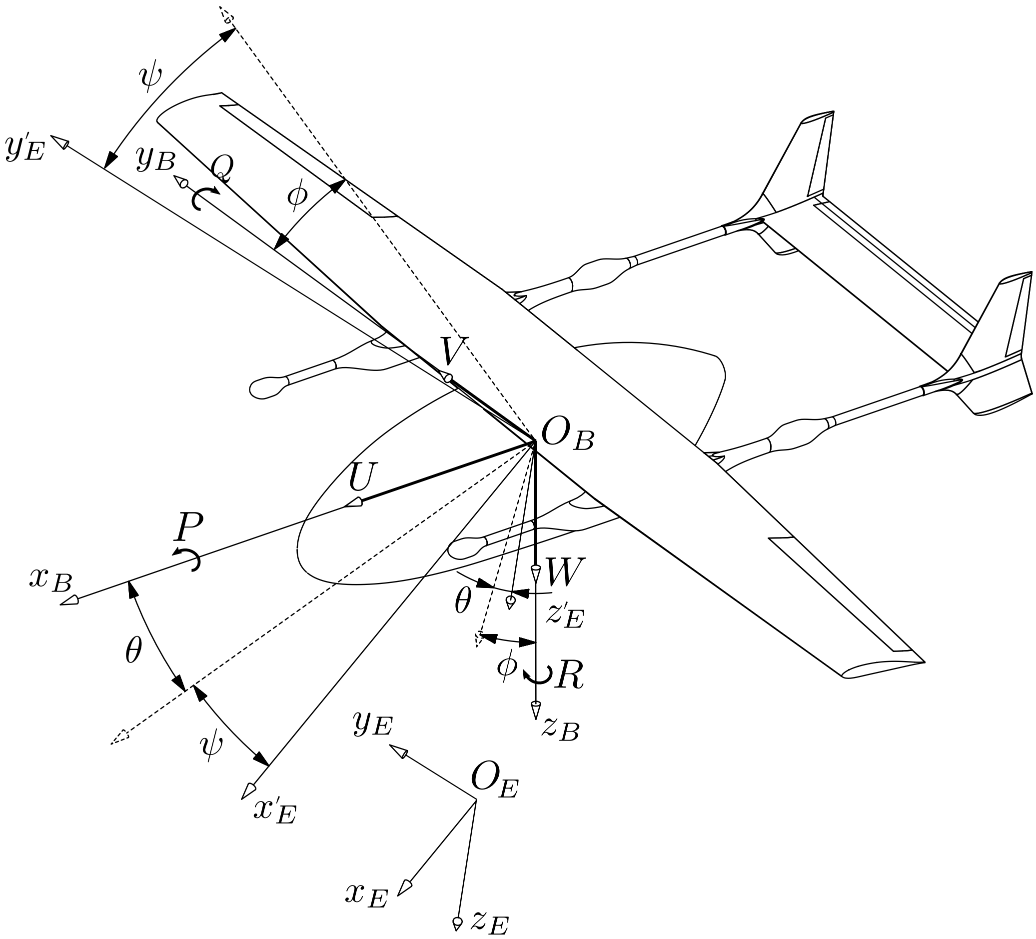

Figure 1 – Body and Earth coordinate systems. Euler angles.

The first step in posing an optimal control problem to calculate the energy-optimal transition trajectory is to derive a mathematical model of the quad-plane motion, valid in the transition phase. The equations of motion have been derived for the coordinate systems specified in figure 1, which are in accordance with most aircraft dynamics sources [14, 15].

The aerodynamic data has been calculated using computational fluid dynamics for angles of attack within the range of -90° to 90° and sideslip angles within the range of -90° to 90°. The propulsion system has been modeled based on the results obtained from the wind tunnel tests and propeller characteristics database. Figure 2 shows the propulsion system of the quad-plane aircraft and coordinate systems used in the analysis. It consists of four coaxial propeller pairs, and one pusher propeller.

The forces and moments of the propulsion system in body frame can be described as

$$\boldsymbol{F_T} = \boldsymbol{T}_{Bm} + \sum_{i=1}^{8} \boldsymbol{T}_{Bvi} \tag{1}$$

$$\boldsymbol{M_T} = \boldsymbol{M}_{Bm} + \boldsymbol{M}_{Bvi} + \boldsymbol{r_m} \times \boldsymbol{T}_{Bm} + \sum_{i=1}^{8} \boldsymbol{r}_{vi} \times \boldsymbol{T}_{Bvi} \tag{2}$$

where vertical i-motor force arm is $\boldsymbol{r}_{vi} = [x_{vi}, y_{vi}, z_{vi}]^T$ and pusher motor force arm is $\boldsymbol{r}_m = [x_m, y_m, z_m]^T$. The distances are measured from aircraft centre of mass to shaft of each motor. Subscript $(.)_{vi}$

represents i-th propeller, and $(.)_m$ - the pusher propeller. $\boldsymbol{T}_{Bm}$, $\boldsymbol{T}_{Bvi}$, $\boldsymbol{M}_{Bm}$ and $\boldsymbol{M}_{Bvi}$ are propeller forces and moments in aircraft body coordinate system, derived from propeller-specific forces and moments in propeller coordinate frames. The pusher propeller forces were modeled after the APC propeller database [16] with the assumption of pure axial flow, and the vertical based on wind tunnel tests of propellers at incidence and analysis of the results [17]. The vertical propulsion model was extended based on an intuitive approach and on basic propeller theory. The vertical, horizontal forces and pitching moment are shown in figure 3 presented in aircraft body frame. The y-axis moment has been derived as an impact of the whole propulsion system on the aircraft body, averaged and divided to show the magnitude for each of the propellers. The existence of the pitching moment is due mostly to uneven conditions and thrust between front and rear propellers. The presented model is interpolated between flight speeds and expected to be exact only in the low range of angles of attack, and approximate in the extended region. Moreover, high uncertainty is expected in the high positive angle of attack range, where vortex ring state can occur. The trajectory however happens predominantly in negative angles of attack, therefore this effect is not expected to largely influence the results.

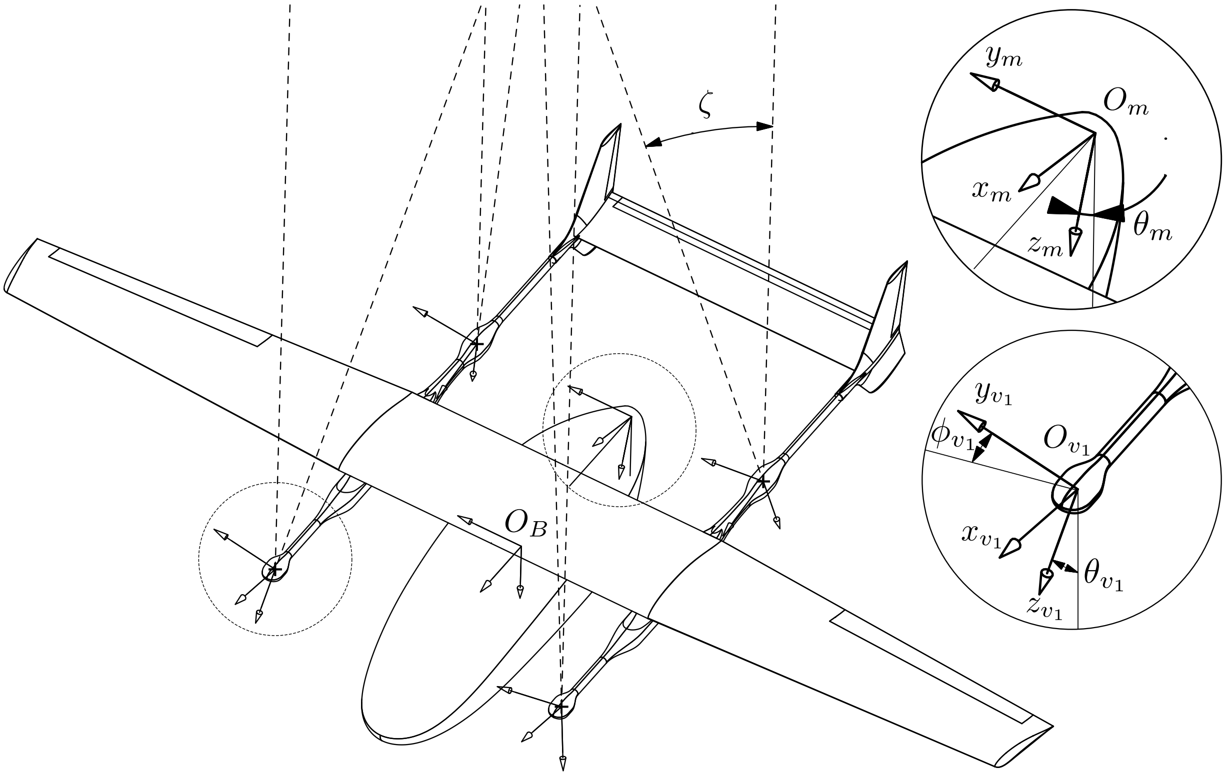

Figure 2 – Propulsion system geometry. Propeller coordinate systems.

The dynamics of BLDC motors are often assumed as first order [18] as in equation 3.

$$\frac{u_i(s)}{\tau_i(s)} = \frac{u_m(s)}{\tau_m(s)} = \frac{K}{Ts+1} \tag{3}$$

The mathematical model has been implemented in MATLAB. Based on it, an optimal control problem has been formulated and solved.

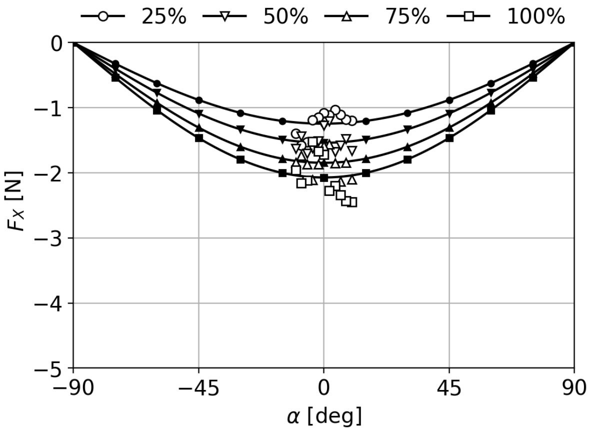

(a) Tail-boom body x force for wind speed of 10 m/s (extended model).

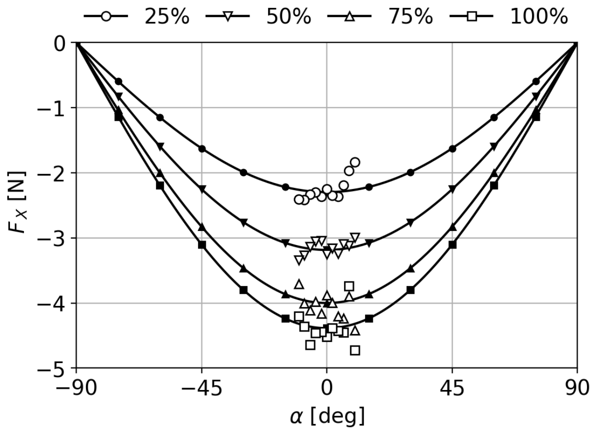

(b) Tail-boom body x force for wind speed of 20 m/s (extended model).

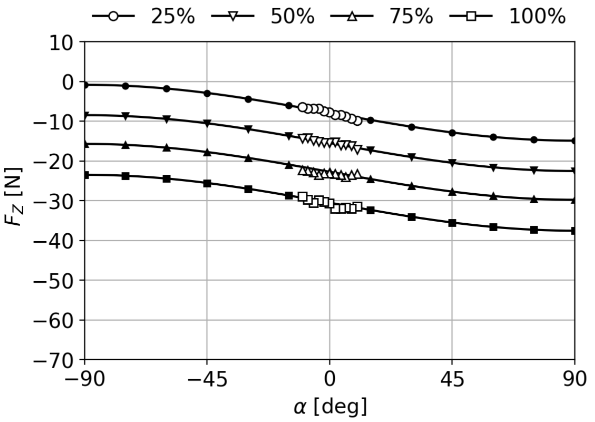

(c) Tail-boom body z force for wind speed of 10 m/s (extended model).

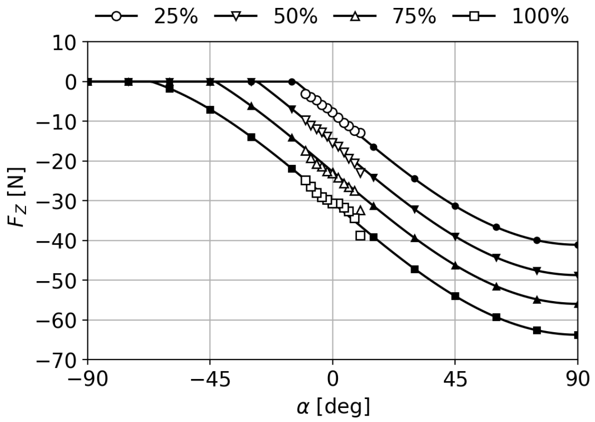

(d) Tail-boom body z force for wind speed of 20 m/s (extended model).

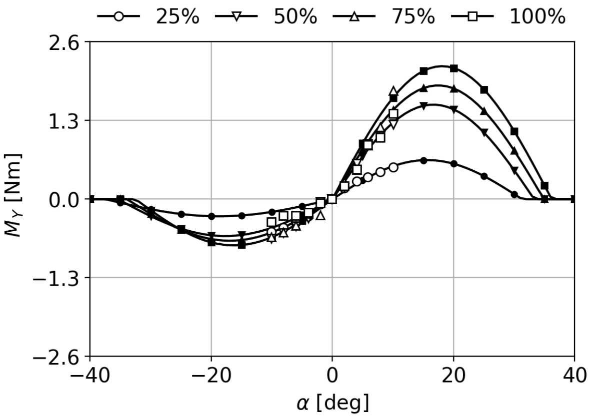

(e) Tail-boom body y moment for wind speed of 10 m/s without 0 AoA correction (extended model).

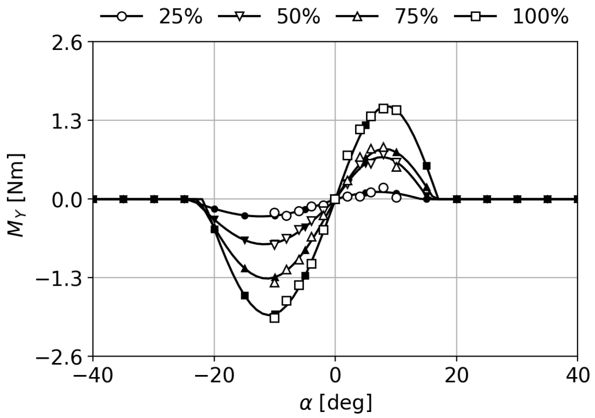

(f) Tail-boom body y moment for wind speed of 20 m/s without 0 AoA correction (extended model).

Figure 3 – Comparison between wind tunnel results and the extended model for two flight speeds and variable angle of attack - vertical force and moment equilibrium. The results are for a single propeller, and the subscript i has been dropped. Wind tunnel results from [17]

The final stage of the numerical model derivation concerns the power and energy required for the vehicle. These quantities will be employed in deriving the optimal trajectory from the standpoint of minimising energy expenditure during the transition phase. The power necessary for the flight of a vertical take-off and landing (VTOL) aircraft can be expressed as a sum of induced P_i, profile P_p and parasitic power P_c.

$$P = P_i + P_p + P_c \tag{4}$$

And the components can be written as

$$P_i = \sum_{i=1}^{8} \frac{T_{vi}^{3/2}}{\sqrt{2\rho A_{vi}}} f(\sqrt{\bar{u_{vi}}^2 + \bar{v_{vi}}^2}) + \frac{T_m^{3/2}}{\sqrt{2\rho A_m}} f(\sqrt{\bar{w_m}^2 + \bar{v_m}^2}) \tag{5}$$

$$P_p = \sum_{i=1}^{8} \frac{1}{64} \rho c_{vi} C_{Dvi} \omega_{vi}^3 D_{vi}^4 + \frac{1}{64} \rho c_m C_{Dm} \omega_m^3 D_m^4 \tag{6}$$

$$P_c = \sum_{i=1}^{8} T_{vi} w_{vi} + T_m u_m \tag{7}$$

2.2 Optimal Control Problem Statement

2.2.1 Nonlinear optimal control with collocation

The objective of optimal control theory is to identify a control sequence, or preferably a control law, which will optimally guide the plant through a range of states in accordance with a specified objective function. For a dynamic model governed by equation

$$\dot{x} = f(x, u, t) \tag{8}$$

With the performance measure in the general form of

$$J = h(x_f, t_f) + \int_{t_0}^{t_f} g(x, u, t)\, dt \tag{9}$$

The calculated admissible control $u^*(t)$ and trajectory $x^*(t)$ are called optimal. The global minimum of a performance measure, denoted by J^* is achieved for an optimal control sequence that belongs to a set of admissible controls of system f.

$$J^* = J^*(x^*(t), u^*(t), t) \leq J \tag{10}$$

Desirable is to find a functional for control $u^* = g(x(t), t)$. It is then called a control law. The optimal trajectory can be found by solving an optimal control problem numerically, either with a direct or an indirect optimal control approach [19]. The method used in this study is the direct approach based on collocation, in which the original OCP is disretized and transcribed to a finite-dimensional static optimization problem, which can then be solved by a large-scale optimization solver. The chosen polynomial collocation scheme was the third order Hermite-Simpson.

2.2.2 Linear Quadratic Regulator

The LQR is one of the specific cases in which an analytical solution to the OCP exists. Moreover, it is a valid control method used in UAV transition control [20]. The objective is

$$J = \frac{1}{2}\boldsymbol{x}^T(t_f) H \boldsymbol{x}(t_f) + \frac{1}{2}\int_{t_0}^{t_f} \left(\boldsymbol{x}^T(t) Q \boldsymbol{x}(t) + \boldsymbol{u}^T(t) R \boldsymbol{u}(t)\right) dt \tag{11}$$

with Q and H positive semi-definite, symmetric matrices, and R positive definite symmetric matrix, subject to a linear, time-invariant system of the form

$$\dot{\boldsymbol{x}}(t) = A\boldsymbol{x}(t) + B\boldsymbol{u}(t) \tag{12}$$

The solution to the LQR problem is

$$\boldsymbol{u}^*(t) = -K(t)\boldsymbol{x} \tag{13}$$

The result is a full state feedback control law, therefore either the measurement of every system state is required, or an additional observer to reconstruct the state from available output. In the case of the highly nonlinear model as presented in this paper, a different approach is using a gain-scheduled LQR for a time-varying system of the form

$$\dot{\boldsymbol{x}}(t) = A(t)\boldsymbol{x}(t) + B(t)\boldsymbol{u}(t) \tag{14}$$

The linear time-varying system derived from the nonlinear model presented in preceding chapters can be obtained through linearization along the selected trajectory. It is of high importance to ensure that the states do not diverge significantly from the linearization points in order to prevent the generation of substantial errors in the linear formulation with respect to the nonlinear model. The points were selected to align with the time mesh utilized for trajectory optimization. This approach resulted in a reduced computational time for linear gain-scheduling during simulation and demonstrated favorable outcomes in command tracking during nonlinear simulation. Furthermore, the simulation and controller were conducted with continuous models, necessitating the use of linear interpolation to maintain continuity. Next, in each of the trajectory points and for all the corresponding models, a control gain matrix has been calculated based on the Q and R matrices chosen for the full duration of the maneuver in LQR formulation to arise at a compromise between control inputs magnitudes and values of error between the state and the trajectory. The goal was good trajectory tracking in the longitudinal plane, while maintaining low regulation errors in the lateral states, and avoid actuator saturation as much as possible. The matrices selected after a trial and error procedure were

$$\begin{aligned} Q &= diag(10\ 10^4\ 5\cdot 10^3\ 5\cdot 10^2\ 3.5\cdot 10^3\ 5\cdot 10^2\ 0\ 4.5\cdot 10^3\ 0\ 1\ 10\ 0\ 0\ 0\ 0\ 0\ 0\ 0\ 0\ 0\ 0) \\ R &= diag(100 \quad 10 \quad 10 \quad 8.5 \quad 8.5 \quad 8.5 \quad 8.5 \quad 8.5 \quad 8.5 \quad 8.5 \quad 8.5 \quad 8.5) \end{aligned} \tag{15}$$

for an LTV system with the state and control vectors

$$\boldsymbol{x}(t) = [V_\infty, \alpha, \beta, P, Q, R, \phi, \theta, \psi, x_E, y_E, H, u_{v1}, u_{v2}, u_{v3}, u_{v4}, u_{v5}, u_{v6}, u_{v7}, u_{v8}, u_m]^T \tag{16}$$

$$\boldsymbol{u}(t) = [\delta_e, \delta_a, \delta_r, \tau_{v1}, \tau_{v2}, \tau_{v3}, \tau_{v4}, \tau_{v5}, \tau_{v6}, \tau_{v7}, \tau_{v8}, \tau_m]^T \tag{17}$$

3. Solution to the OCP

The optimal control problem has been transcribed into a static optimization problem with the use of collocation in ICLOCS2 MATLAB toolbox [21]. Optimal trajectory and control has been found with IPOPT solver [22]. The following section shows the optimized trajectories for the presented mathematical model, and the linear-quadratic control system design.

3.1 Zero-pitch reference

In order to establish a baseline for comparison of the optimisation results, a reference transition scenario was devised as follows: upon reaching a specified transition altitude, the aircraft commences acceleration using predominantly horizontal propulsion. The aircraft maintains a pitch angle of approximately zero degrees. The vertical position is maintained by the thrust of the vertical propellers. The thrust of the vertical propellers is gradually reduced to zero when the aerodynamic forces generated by the wings begin to support the weight of the aircraft (stall speed). The altitude was not constrained during the maneuver to allow for variations in angle of attack and maintain a zero pitch angle. However, the deviations in altitude were not significant. The objective for deriving zero pitch trajectory was

$$J = \int_0^{t_f} \theta(t)^2\, dt \tag{18}$$

The energy consumption for this case was 92551.0 J, with a transition time from hover to horizontal flight of 23.63 seconds and an altitude of 200.55 metres.

3.2 Energy-optimal transition and control system design

Below are shown results from optimization of energy consumption with the assumption of a free altitude during transition, and a feedback control system design to track the resulting energy-optimal trajectory for an offline control application. A simple gain-scheduled LQR was selected in this phase of the research. Its simple structure can be seen in figure 4. The objective function for trajectory calculations is

$$J = \int_0^{t_f} P(t)\,dt \tag{19}$$

where $P(t)$ is the power of flight according to equation 7. The tracking simulation was done for a six degree-of-freedom model to test the assumptions and feasibility of the three degree-of-freedom trajectory for the full model. Moreover, to simulate a more realistic case, for the purposes of tracking a first-order model of motor dynamics was introduced. The optimal trajectory was recalculated after introducing additional motor states to the model. Figure 5 shows the resulting longitudinal trajectory and the tracking results. In figure 6 are the lateral state variables regulated to zero. In this case, the altitude was kept free during the maneuver, and fixed in the beginning and at the end of transition at 300 meters. The lowest value of altitude reached $298.2\mathrm{m}$. The resulting trajectory consists of a pitch-down motion to about -40° after about $0.5\mathrm{s}$, with pitch rates reaching $-63^\circ\,\mathrm{s}^{-1}$, after which follows a pitch-up back to level flight with up to $35^\circ\,\mathrm{s}^{-1}$. The vehicle speed experiences a rapid rise, followed by a lower acceleration. At the end of transition, the pitch attitude of the vehicle oscillates slightly, and finally reaches the value for forward flight. Transition from hover to horizontal flight took $3.37\mathrm{s}$ and the maneuver finished at $28.74\mathrm{m}$.

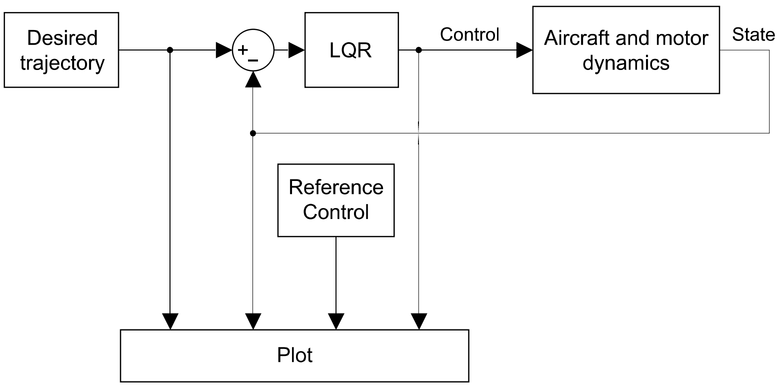

Figure 4 – Gain-scheduled LQR control system architecture for tracking the desired energy-optimal trajectory

The control inputs from the vertical and horizontal propulsion systems, as well as the power and energy utilized during the transition, are illustrated in figures 7 and 8. At the outset of the maneuver, the rear propellers provide additional thrust to facilitate pitch-down motion. Subsequently, the roles of the rear and front motors are exchanged, with a higher throttle value applied to the front motors to restore the pitch angle to positive values. As the pitch angle decreases, the throttle of the pusher motor is reduced in order to diminish its impact on the pitch-down moment and to maintain a constant altitude. Once a more level flight has been achieved, the throttle of the pusher motor is returned to the highest allowable value in order to accelerate the vehicle more rapidly and thereby reduce the energy consumed. As anticipated, at the conclusion of the transition, the throttle to the vertical motors is significantly reduced, and the low throttle setting at the rear motors is employed to maintain the desired pitch attitude. The maximum power output was observed to be $15\mathrm{kW}$. The energy consumption for this case was found to be $26559.0\mathrm{J}$.

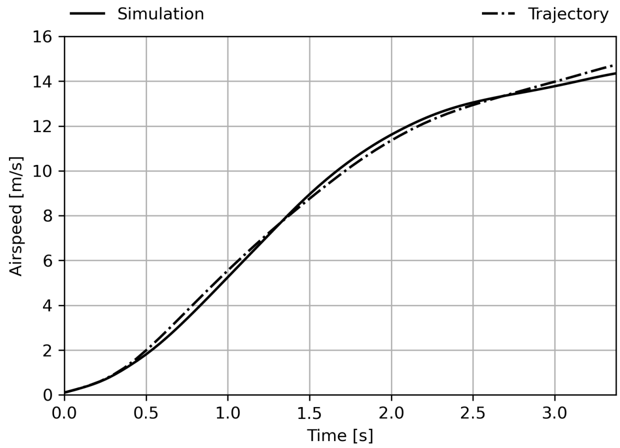

(a) Airspeed tracking

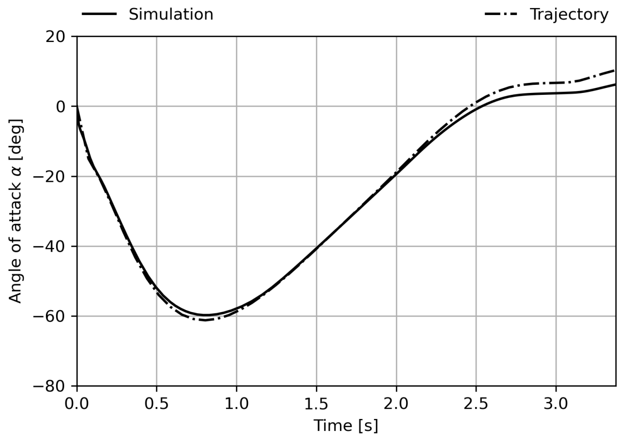

(b) Angle of attack tracking

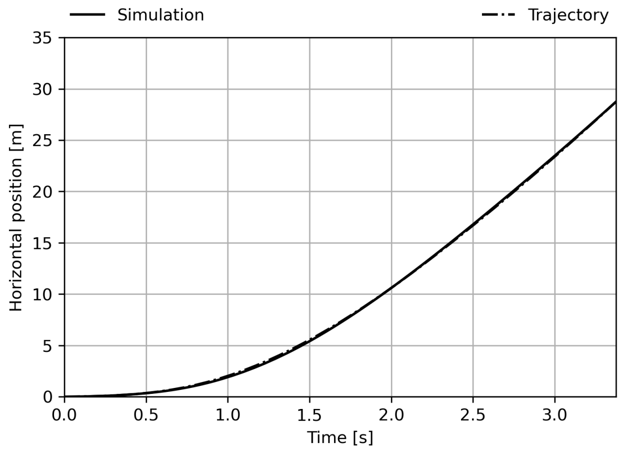

(c) Horizontal position tracking

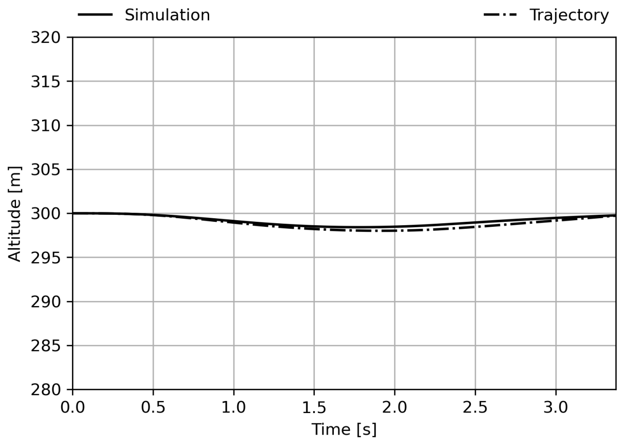

(d) Altitude tracking

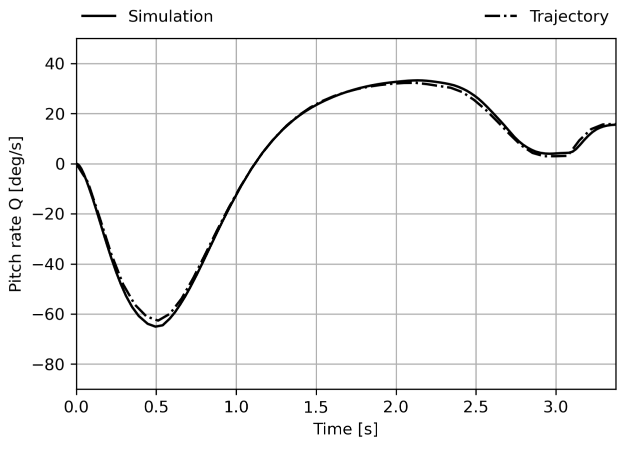

(e) Pitch rate tracking

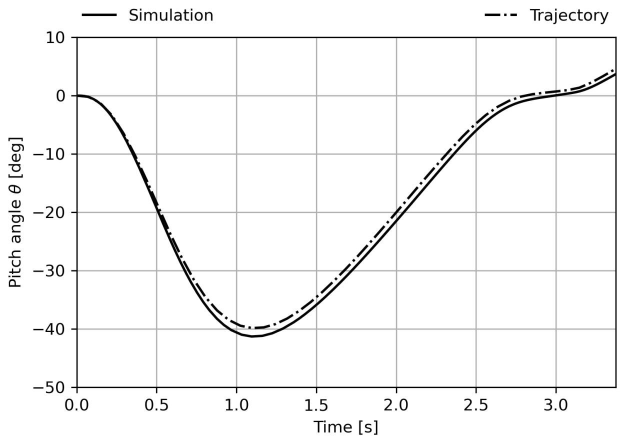

(f) Pitch angle tracking

Figure 5 – Comparison of state variables (longitudinal) in tracking a reference trajectory by an LQR (with motor dynamics modeled).

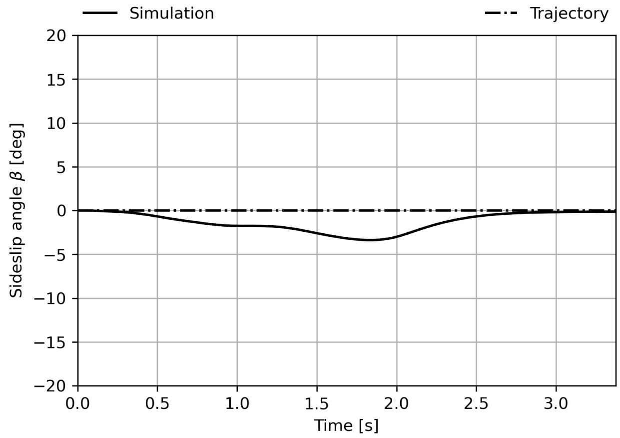

(a) Sideslip angle tracking

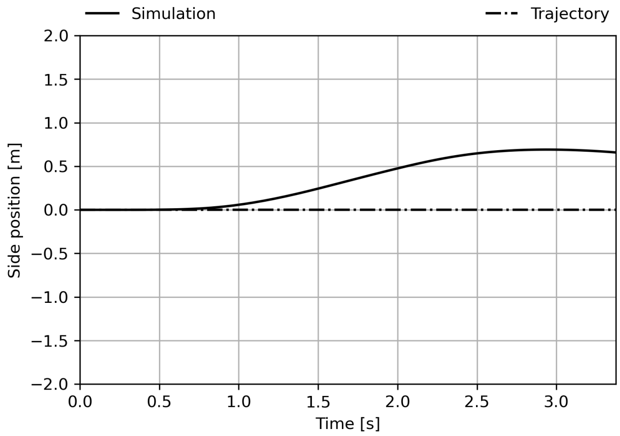

(b) Side position tracking

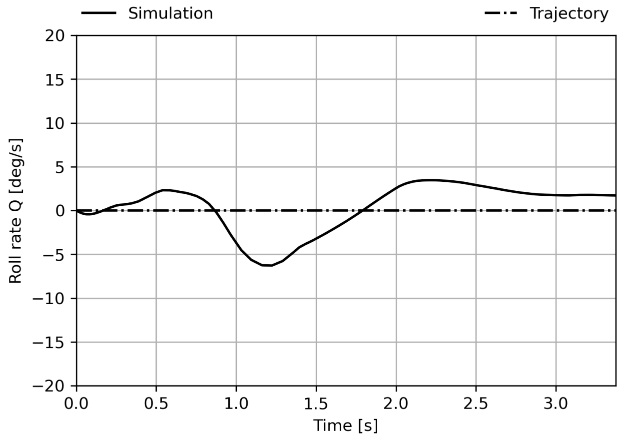

(c) Roll rate tracking

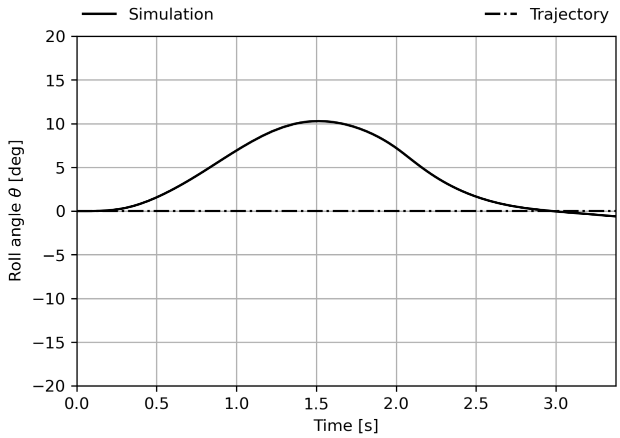

(d) Roll angle tracking

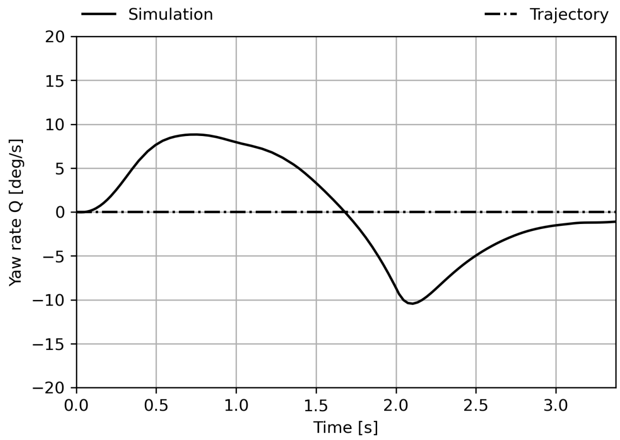

(e) Yaw rate tracking

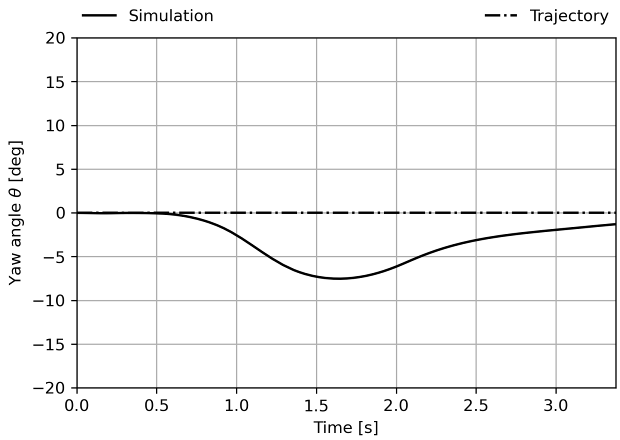

(f) Yaw angle tracking

Figure 6 – Comparison of state variables (lateral) in tracking a reference trajectory by an LQR (with motor dynamics modeled)

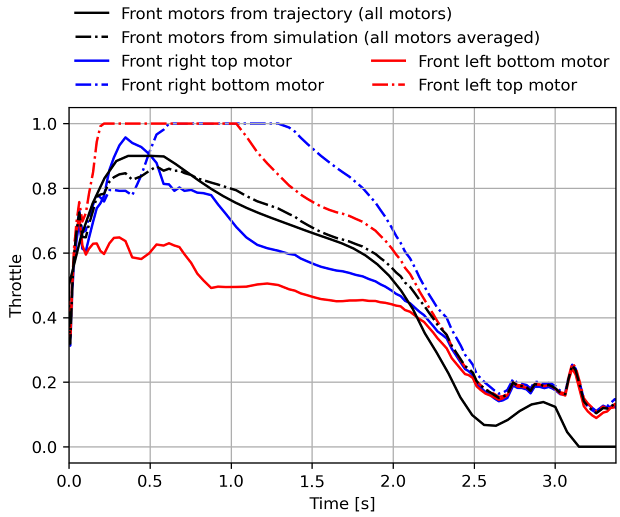

(a) Front motors throttle

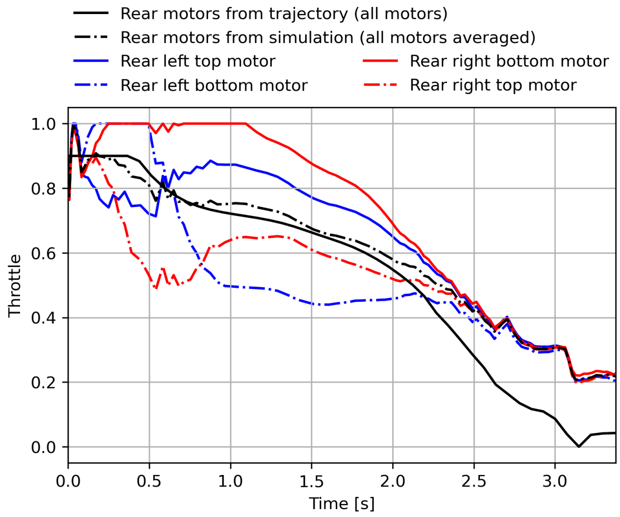

(b) Rear motors throttle

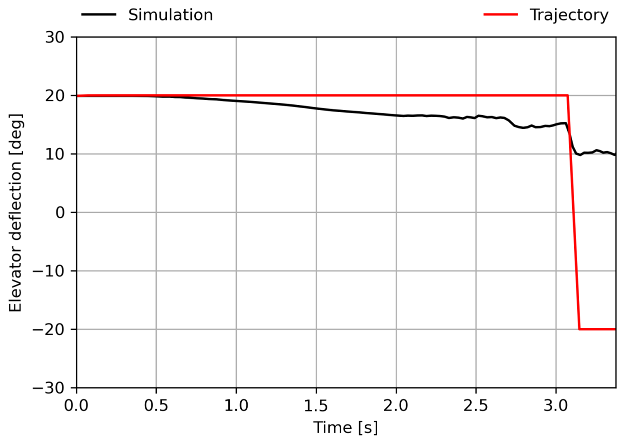

(c) Elevator deflection

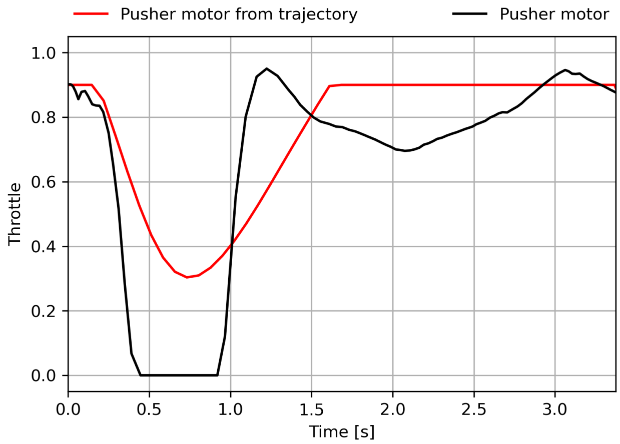

(d) Pusher motor throttle

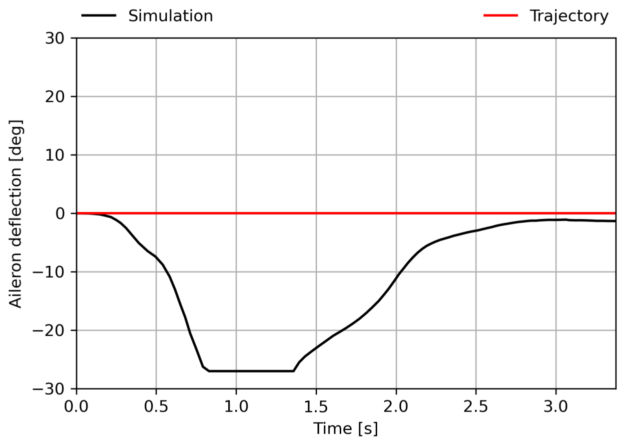

(e) Aileron deflection

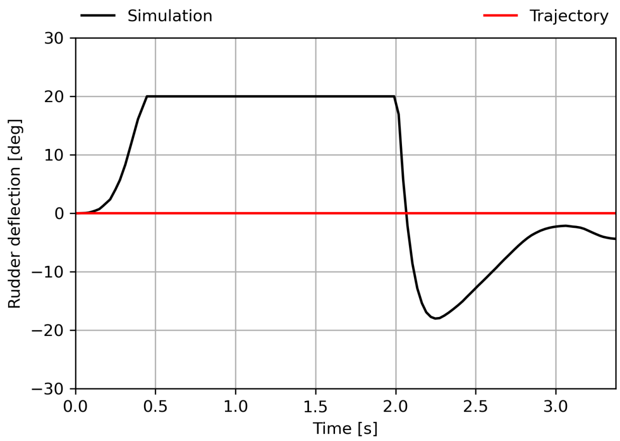

(f) Rudder deflection

Figure 7 – LQR automatic control in energy-optimal trajectory tracking (with motor dynamics modeled)

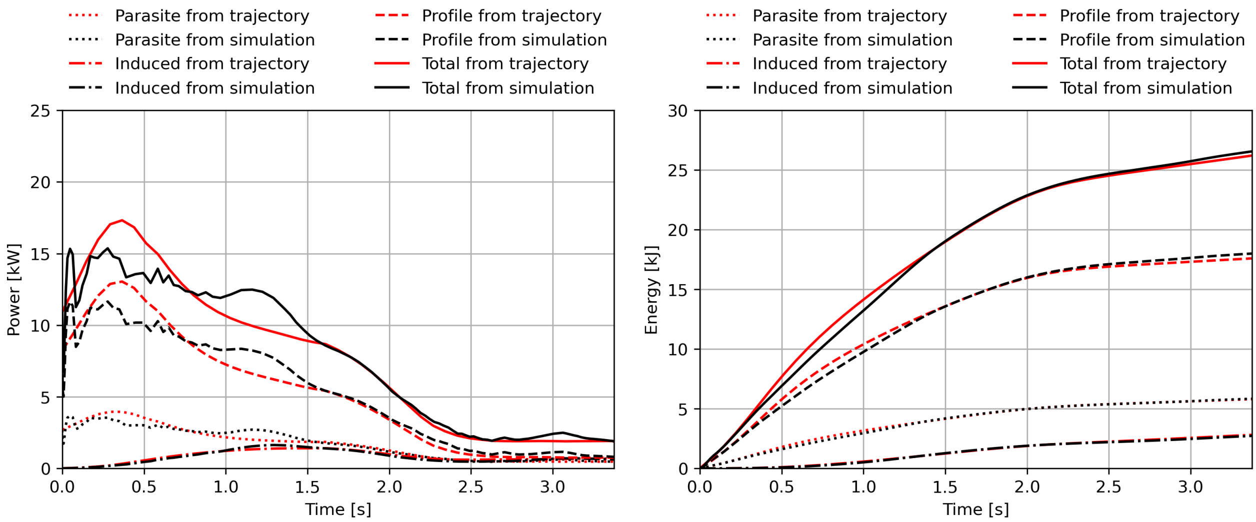

(a) Motor power

(b) Motor energy consumption

Figure 8 – Comparison of ideal trajectory power and energy, and power and energy consumed by the controller (with motor dynamics modeled)

An important conclusion from the considerations was that it was impossible to use a model with motor dynamics included to track a reference derived for a model without this component. This result was also evident in the attempt of adding a dynamic estimator to track a trajectory derived without it, which resulted in the original trajectory being unfeasible for the augmented control system.

Nevertheless, the objective of the section, namely the design of a control system for the quad-plane to track the energy-efficient transition trajectory, was demonstrated to be attainable through the utilisation of a feedback control system. Furthermore, the incorporation of the feedback controller and lateral states into the 6-degree-of-freedom simulation did not result in a notable increase in energy consumption, despite the lateral states not being regulated optimally. Consequently, the efficacy of feedback control in tracking the transition trajectory of a quad-plane and maintaining energy savings was validated.

4. Conclusions

In light of the findings of the trajectory optimization, it is possible to draw two significant conclusions. In order to enhance energy efficiency during flight, it is imperative to minimize the time spent in hovering and during transition. The second conclusion is that controlled pitching downwards of the aircraft was found to be beneficial in reducing energy consumption. Even though the resulting trajectory was quick, aggressive and required large bursts of power, the energy of maneuver was largely decreased of about 70% less then the reference trajectory. The trajectory calculations were performed without any requirements for stall avoidance and forward acceleration limits. This approach is valid for uncrewed applications. However, if this approach is to be used for Urban Air Mobility crewed applications, the OCP would need to be augmented with constraints for passenger comfort and safety, as the trajectories obtained without such constraints yielded a quite aggressive transition.

Comparison of the resulting trajectories is shown in table 1. The data demonstrates that optimizing the trajectory of the transition phase is an invaluable tool for reducing the energy consumption of a VTOL. Furthermore, the duration and distance of the transition phase are reduced, making the vehicle capable of accelerating and retreating at a faster rate in scenarios where time and space are limited. In addition, the optimization of the transition phase allows for take-off in more confined spaces and in time-sensitive operations. Examples of such scenarios can be found in rural operations (parcel delivery, air taxis, surveillance), as well as military applications. In such circumstances, the time taken for the vehicle to be identified by an enemy is of the essence and should be kept to a minimum to circumvent detection and the subsequent deployment of countermeasures.

It can be observed from the results that the final transition speed could have been selected slightly larger, as the vertical propulsion system was still operational at the conclusion of the transition, de-

Case	Energy [J]	Time [s]	Distance [m]	Savings [%]
Zero-pitch Reference	92551.0	23.63	200.55	-
Minimum Energy - Trajectory	26413.1	3.59	31.89	71.46
Minimum Energy - Tracking	26559.0	3.37	28.74	71.30

Table 1 – Comparison of results.

spite the fact that the wings should have been capable of providing the entirety of the vertical force. Furthermore, the aircraft was not yet in pitch equilibrium, as there was a discrepancy between the front and rear motor inputs in all cases. However, the value of the control input at the conclusion of the transition was minimal, representing approximately 10% of the throttle range, and contributed only a fraction of the total vertical force. Consequently, it was not a substantial deviation, but could potentially influence the transition between transition and horizontal flight, as some transient, unsteady effects may be anticipated. The next issue is the saturation of the control input at the outset of the transition is an unfavourable characteristic, and was caused by the selection of constraints for the transition trajectory. It was assumed that the motors could utilise up to 90% of their potential range, leaving 10% of the range unoccupied. The margin of the motor inputs that was left has been demonstrated to be inadequate for tracking the derived trajectory, regulating the lateral states, and avoiding saturation in some motors. Therefore, more attention should be paid in proper selection of this margin.

5. Contact Author Email Address

Mail to: katarzyna.pobikrowska.dokt@pw.edu.pl or tomasz.grabowski@pw.edu.pl

6. Copyright Statement

References

[1] Yasmina Bestaoui Sebbane. *SMART AUTONOMOUS AIRCRAFT: Flight Control and Planning for UAV*. CRC PRESS, Boca Raton, Florida, 2020.

[2] Philipp Foehn, Angel Romero, and Davide Scaramuzza. Time-optimal planning for quadrotor waypoint flight. *Science Robotics*, 6(56):1–19, July 2021.

[3] F. Nex, C. Armenakis, M. Cramer, D.A. Cucci, M. Gerke, E. Honkavaara, A. Kukko, C. Persello, and J. Skaloud. UAV in the advent of the twenties: Where we stand and what is next. *ISPRS Journal of Photogrammetry and Remote Sensing*, 184:215–242, February 2022.

[4] EASA. Study on the Societal Acceptance of Urban Air Mobility in Europe. Technical report, May 2021.

[5] Information Resources Management Association, editor. *Unmanned Aerial Vehicles: Breakthroughs in Research and Practice*. IGI Global, 2019.

[6] Jacek Mieloszyk. Numerical multidisciplinary optimization of aircraft with flight dynamic stability constraints. *Proceedings of the Institution of Mechanical Engineers, Part G: Journal of Aerospace Engineering*, 235(1):70–80, January 2021.

[7] Tomasz Goetzendorf-Grabowski. Flight dynamics of unconventional configurations. *Progress in Aerospace Sciences*, 137(100885), February 2023.

[8] Tomasz Goetzendorf-Grabowski. Multi-disciplinary optimization in aeronautical engineering. *Proceedings of the Institution of Mechanical Engineers, Part G: Journal of Aerospace Engineering*, 231(12):2305–2313, May 2017.

[9] Sudath Munasinghe and A. A. J. K. Gunarathna. Comparison of Vertical and Bird Take-off Methods of Quad-Plane Miniature Aerial Vehicles. Preprint, November 2022.

[10] Tomasz Goetzendorf-Grabowski, Dominika Kacik, Katarzyna Pobikrowska, and Jacek Mieloszyk. Optimization of Energy Consumption in the Transition State of a Quad-Plane. In *Proceedings of 33th INTERNATIONAL CONGRESS OF THE AERONAUTICAL SCIENCES*, pages 1–8, 2022. ICAS 2022-0576.

[11] Tomasz Goetzendorf-Grabowski, Jacek Mieloszyk, Marcin Figat, Andrzej Tarnowski, and Bogdan Hernik. LIGHTWEIGHT UAV FOR EMERGENCY MEDICAL SERVICE. In *Proceedings of 32th INTERNATIONAL CONGRESS OF THE AERONAUTICAL SCIENCES*, pages 1–11, 2021. ICAS 2020-0030.

[12] Tomasz Goetzendorf-Grabowski, Andrzej Tarnowski, Marcin Figat, Jacek Mieloszyk, and Bogdan Hernik. Lightweight unmanned aerial vehicle for emergency medical service – Synthesis of the layout. *Proceedings of the Institution of Mechanical Engineers, Part G: Journal of Aerospace Engineering*, 235(1):5–21, January 2021.

[13] Hugo Rodríguez-Cortés, Marco Martínez-Ramírez, and Diego Martínez-Velasco. Autopilot for flight mode transistion in quadplanes. *Memorias del Congreso Nacional de Control Automático*, 6(1):568–573, October 2023.

[14] Wayne Durham. *Aircraft Flight Dynamics and Control*. Wiley, Chichester, West Sussex, 2013.

[15] Marcello R. Napolitano. *Aircraft Dynamics: From Modeling to Simulation*. J. Wiley, Hoboken, New Jersey, 2012.

[16] APC Propellers - Performance Data. `https://www.apcprop.com/technical-information/performance-data/`.

[17] Katarzyna Pobikrowska and Tomasz Goetzendorf-Grabowski. Wind tunnel tests of hovering propellers in the transition state of Quad-Plane. *Bulletin of the Polish Academy of Sciences Technical Sciences*, 69(6):e138821, September 2021.

[18] Gabriel M. Hoffmann, Haomiao Huang, Steven L. Waslander, and Claire J. Tomlin. Precision flight control for a multi-vehicle quadrotor helicopter testbed. *Control Engineering Practice*, 19(9):1023–1036, September 2011.

[19] Anil V. Rao. A survey of numerical methods for optimal control. In *AAS/AIAA Astrodynamics Conference*, volume 135, pages AAS 09–334, Pittsburgh, Pensylwania, August 2009. American Astronautical Society.

[20] P. Casau, D. Cabecinhas, and C. Silvestre. Transition Control for a fixed-wing Vertical Take-Off and Landing Aircraft. *IFAC Proceedings Volumes*, 44(1):7250–7255, January 2011.

[21] Yuanbo Nie, Omar Faqir, and Eric C. Kerrigan. ICLOCS2: Try this Optimal Control Problem Solver Before you Try the Rest. In *2018 UKACC 12th International Conference on Control (CONTROL)*, pages 336–336, Sheffield, September 2018. IEEE.

[22] Andreas Wächter and Lorenz T. Biegler. On the implementation of an interior-point filter line-search algorithm for large-scale nonlinear programming. *Mathematical Programming*, 106(1):25–57, March 2006.